

The Hubble Tension Revisited: Additional Local Distance Ladder Uncertainties

EDVARD MÖRTSELL,¹ ARIEL GOOBAR,¹ JOEL JOHANSSON,¹ AND SUHAIL DHAWAN²

¹*Oskar Klein Centre, Department of Physics, Stockholm University
Albanova University Center
106 91 Stockholm, Sweden*

²*Institute of Astronomy
University of Cambridge Madingley Road
Cambridge CB3 0HA
United Kingdom*

ABSTRACT

In a recent paper, we argued that systematic uncertainties related to the choice of Cepheid color-luminosity calibration may have a large influence on the tension between the Hubble constant as inferred from distances to Type Ia supernovae and the cosmic microwave background as measured with the Planck satellite. Here, we investigate the impact of other sources of uncertainty in the supernova distance ladder, including Cepheid temperature and metallicity variations, supernova magnitudes and GAIA parallax distances. Excluding Milky Way Cepheids based on parallax calibration uncertainties, for the color excess calibration we obtain $H_0 = 70.8 \pm 2.1$ km/s/Mpc, 1.6σ from the Planck value.

Keywords: Cepheid distance (217), Hubble constant (758), Type Ia supernovae (1728), Interstellar dust extinction (837)

1. INTRODUCTION

Cepheid stars are crucial in building up the distance ladder to Type Ia supernovae (SNIa) when estimating the Hubble constant H_0 . To be used as standard candles, Cepheids need to be calibrated with respect to fact that

- long period Cepheids are brighter,
- red Cepheids are dimmer,
- and Cepheids in high metallicity environments are brighter.

The Cepheid color-luminosity (C-L) correlation may be understood as a combination of extrinsic dust extinction and intrinsic temperature variations (Pejcha & Kochanek 2012). Given the difficulty in separating these effects, Cepheids are usually calibrated using a phenomenological approach where a parameter, R , corrects for both dust and intrinsic variations

(Madore 1982). The correction can be applied to observed colors, as by the SH0ES team in e.g. Riess et al. (2016), or estimated color excesses, as in Follin & Knox (2018), derived by subtracting a model for the mean intrinsic Cepheid color. Regardless of which method is employed, it will by necessity correct for both extrinsic and intrinsic color variations since the observed color and estimated color excess only differ by a linear term depending on the Cepheid period. When assuming a global value for R , the choice of calibration method is of minor importance since only the difference between Cepheid magnitudes in anchor and SNIa host galaxies matters for the H_0 inference. When allowing for the calibration parameter to vary between galaxies, motivated by the observed variation in dust properties (Mortzell et al. 2021), the choice of calibration method makes a substantial difference. As demonstrated in Mortzell et al. (2021), using Wesenheit H-band magnitudes calibrated with respect to the observed color $R_W(V - I)$ where R_W is allowed to vary between galaxies gives $H_0 = 66.9 \pm 2.5$ (in units of km/s/Mpc implied from now on), whereas calibrating using estimated color excesses $R_E \hat{E}(V - I)$ yields $H_0 = 71.8 \pm 1.6$, a

2.7σ tension with the value inferred from the cosmic microwave background (CMB) observations with the Planck satellite (Aghanim et al. 2020). Presenting the largest tension with the Planck value, and arguably being closest to a physical Cepheid model as presented in Pejcha & Kochanek (2012), throughout the paper, we will use the color excess calibration as our default method for investigation.

We first investigate the impact of Cepheid temperature variations on the inferred H_0 uncertainty and discuss how systematic effects connected to the metallicity calibration may shift the inferred H_0 and increase the error budget. We then show that the local Cepheid calibrated SNIa magnitude uncertainties may be underestimated and express concerns about the reliability of the Milky Way (MW) Cepheid parallax distance calibration.

We finally point out that the Cepheid color excess distributions have substantial variations between galaxies, and that the inferred H_0 is sensitive to the introduction of color cuts in the data.

2. METHOD AND DATA

2.1. Cepheid Calibration

We use the Hubble Space Telescope (HST) near-infrared flux ($H = F160W$), color calibrated using optical ($V = F555W$ and $I = F814W$) data, to derive

$$m_H^W \equiv m_H - R_E \hat{E}(V - I). \quad (1)$$

Here, $\hat{E}(V - I)$ represents a proxy for the color excess $E(V - I) \equiv A_V - A_I = (V - I) - (V - I)_0$, with $(V - I)_0$ the intrinsic Cepheid color. It is obtained by subtracting an estimate of the mean intrinsic colors, $\langle V - I \rangle_0$ from the observed colors. We use mean intrinsic colors from Tammann et al. (2011), including the quoted uncertainties and a 0.075 dispersion in the mean intrinsic Cepheid color between galaxies, from the difference between Large Magellanic Cloud (LMC) and MW Cepheids. These colors are in good agreement with results in Pejcha & Kochanek (2012). We fit for the values of R_E that minimize the scatter in m_H^W .

The Wesenheit magnitude of the j th Cepheid in the i th galaxy, including the anchor galaxies MW, NGC 4258 and the Large Magellanic Cloud (LMC), is modeled as

$$m_{H,i,j}^W = \mu_i + M_H^W + b_W[P]_{i,j} + Z_W[M/H]_{i,j}, \quad (2)$$

with $[M/H]_{i,j}$ the Cepheid metallicity, $[P]_{i,j} \equiv \log P_{i,j} - 1$ where $P_{i,j}$ is the period measured in days, M_H^W the absolute Cepheid magnitude normalized to a period of $P = 10$ days and Solar metallicity and μ_i the distance

modulus to the i th galaxy. We use separate P-L relations for short and long period Cepheids

$$b_W[P]_{i,j} \rightarrow b_W^S[P]_{i,j}^S + b_W^L[P]_{i,j}^L, \quad (3)$$

where $[P]_{i,j}^S = 0$ for Cepheids with periods > 10 days and $[P]_{i,j}^L = 0$ for Cepheids with periods < 10 days.

2.2. Type Ia Supernovae

The apparent SNIa B-band peak magnitude in the i th host, corrected for the width-luminosity and C-L relations using the SALT2 model (Guy et al. 2007), is modeled by

$$m_{B,i} = \mu_i + M_B. \quad (4)$$

The errors on $m_{B,i}$ include the fitting uncertainty and a 0.1 magnitude contribution to take into account the intrinsic SNIa dispersion added in quadrature (Riess et al. 2016; Mortsell et al. 2021).

2.3. Data and Parameter Fitting

For Cepheids in M31 and beyond, we use data from Table 4 in Riess et al. (2016). For Cepheids in the LMC, we use data in Table 2 in Riess et al. (2019). Data for MW Cepheids, including GAIA parallax measurements are from Table 1 in Riess et al. (2021).

20 double eclipsing binaries (DEBs) observed using long-baseline near-infrared interferometry give a distance to the LMC of $\mu_{\text{LMC}} = 18.477 \pm 0.0263$ (Paczynski 1996; Pietrzyński et al. 2019; Riess et al. 2019). Observations of mega-masers in Keplerian motion around its central super massive black hole give a distance to NGC 4258 of $\mu_{\text{LMC}} = 29.397 \pm 0.032$ (Reid et al. 2019).

Type Ia SN B-band magnitudes are from Table 5 in Riess et al. (2016), derived using version 2.4 of SALT II (Betoule et al. 2014).

Given the observed Cepheid magnitudes m_H , color excesses $\hat{E}(V - I)$, periods $[P]$, metallicities $[M/H]$, together with the SNIa magnitudes m_B , the anchor distances μ_k and the MW Cepheid parallaxes π , we fit simultaneously for R_E , b_W , Z_W , the host galaxy distances μ_i , the anchor distances μ_k , the GAIA parallax offset zp , the Cepheid absolute magnitude M_H^W and the SNIa absolute magnitude M_B . Since the system of equations is linear, the fit can be made analytically.

2.4. Default Results for Color excess Calibration

$$R_E \hat{E}(V - I)$$

Allowing for R_E to vary between galaxies, with weak prior constraints on their values $R_E = 0.45 \pm 0.35$, we obtain $H_0 = 71.9 \pm 1.4$ (2.9σ). This is the default result to which we will relate the impact of other systematic effects. Note that the error bars do not yet include the intrinsic Cepheid color scatter, see Section 8.

3. TEMPERATURE VARIATIONS

Given our inability to separate dust and Cepheid temperature color effects, we will here treat the temperature magnitude and color variations as an additional source of uncertainty, following the physical Cepheid model from [Pejcha & Kochanek \(2012\)](#). Denoting the mean temperature deviation for a specific Cepheid by τ , the absolute X-band magnitude will shift according to

$$M_X = \langle M_X \rangle - 2.5\beta_X\tau, \quad (5)$$

where $\langle M_X \rangle$ is the mean absolute magnitude at the specific period, color and metallicity. β_X for a large range of filters are observationally constrained in [Pejcha & Kochanek \(2012\)](#), where also temperature variations are estimated to $\sigma_\tau = 0.02$ given the width of the Cepheid instability strip. The intrinsic color (ic) excess will accordingly be given by

$$\hat{E}_{ic}(V - I) = -2.5(\beta_V - \beta_I)\tau. \quad (6)$$

For each Cepheid, we randomly assign a temperature from $\tau = 0 \pm \sigma_\tau$ and adjust the H-magnitude and color excess according to

$$\begin{aligned} m_H &\rightarrow m_H + 2.5\beta_H\tau \\ \hat{E}(V - I) &\rightarrow \hat{E}(V - I) - \hat{E}_{ic}(V - I), \end{aligned} \quad (7)$$

assuming $\beta_H = 1.72$, $\beta_I = 3.39$ and $\beta_V = 5.14$. The induced impact on the inferred H_0 is estimated generating random Monte Carlo samples, see Section 8. Note that it makes sense treating the temperature color excess as noise for the dust color excess since the former is subdominant, with $\hat{E}_{ic}(V - I) \lesssim 0.1$.

4. METALLICITIES

We correct for metallicity effects on the luminosity using $\delta m_H^W = Z_W[M/H]$, where the bracket is a shorthand notation for

$$\begin{aligned} [M/H] &\equiv \log \left[\frac{(M/H)}{(M/H)_\odot} \right] = \log(M/H) - \log(M/H)_\odot \\ &= \Delta \log(M/H). \end{aligned} \quad (8)$$

In [Riess et al. \(2016\)](#), individual Cepheid metallicities are estimated using $Z = 12 + \log(O/H)$. For LMC Cepheids, a common value of $\Delta \log(O/H) = -0.25$ is used. In [Riess et al. \(2019\)](#), this is updated to $[Fe/H] = -0.3$, referring to [Riess et al. \(2016\)](#) having $[Fe/H] = -0.25$ indicating the identification $[Fe/H] = \Delta \log(O/H)$. However, since

$$[O/H] = [O/Fe] + [Fe/H], \quad (9)$$

this is only true if $[O/Fe] = 0$. As stated in [Israelian et al. \(1998\)](#), all studies agree that $[O/Fe]$ increase when $[Fe/H]$ decrease from 0 to -1 . Approximating this dependence to be linear, $[O/Fe] = k[Fe/H]$, we can write

$$[O/H] = k[Fe/H] + [Fe/H] = [Fe/H](1 + k). \quad (10)$$

Figure 3 in [Amarsi et al. \(2015\)](#) and figure 20 in [Luck \(2018\)](#) suggest that $k \sim -0.5$, with an uncertainty of order $\sigma_k = 0.25$.

When estimating the Cepheid metallicity from iron and oxygen abundances, state-of-art compilations differ by ~ 0.15 in the difference $Z_\odot - Z_\odot^{Fe}$ ([Vagnozzi 2019](#)). In [von Steiger & Zurbuchen \(2015\)](#), a value of $H/O = 1500 \pm 300$ is given, corresponding to $Z_\odot = 8.824 \pm 0.087$ which we will use as our default value but with an 0.15 dispersion to take into account the uncertainty between Cepheid metallicities estimated from oxygen and iron abundances.

4.1. Impact on H_0

The derived H_0 increases slightly with increasing LMC metallicity. A shift $\Delta \log(O/H) = -0.3 \rightarrow -0.25$ increases the inferred Hubble constant with $\delta H_0 \sim 0.07$.

The inferred H_0 depends on k as $\delta H_0 / \delta k \sim -0.7$, and changing from $k = 0$ to $k = -0.5$, we obtain $H_0 = 72.1 \pm 1.4$. A constant systematic shift in the Cepheid metallicities as inferred from iron and oxygen abundances can be parametrized by changing the assumed solar oxygen abundance. An increase δZ_\odot will increase H_0 with $\delta H_0 / \delta Z_\odot \sim 6$. Shifting $Z_\odot = 8.824 \rightarrow 8.674$, for the default case we get $H_0 = 71.3 \pm 1.5$ (2.5σ tension). The full impact on the inferred H_0 is estimated using Monte Carlo techniques in Section 8.

5. SUPERNOVA MAGNITUDE UNCERTAINTIES

If we instead of fitting for a global absolute SNIa magnitude, fit for individual M_B , we obtain one estimate of H_0 for each SNIa, see figure 1. Apart from noting that only a handful of SNIae are in significant tension with the CMB result for H_0 , we also note that the scatter is slightly larger than expected given the individual error bars, possibly indicating underestimated SNIa magnitude uncertainties. Taking the full correlation between the inferred M_B into account, the SNIa error bars should be increased by a factor of 1.13 in order for the $\chi^2/\text{dof} = 1$ assuming the individual M_B have their origin in a common value. Increasing the $\sigma(M_B)$ by this factor, for the default case we obtain $H_0 = 71.9 \pm 1.5$, decreasing the Planck tension slightly to 2.8σ .

5.1. Impact of Type Ia Supernova Data Set

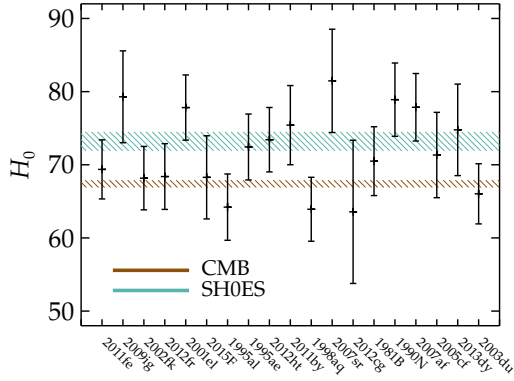


Figure 1. Fitting individual R_E and H_0 with priors $R_E = 0.45 \pm 0.35$.

The fact that the statistical error on H_0 is dominated by SNIa data, and only a sub-set of the SNIa are in tension with the Planck H_0 may raise concerns about the reliability of the individual SNIa magnitude estimates. However, using the SNIa data set from Burns et al. (2018), gives very similar result, indicating that systematic effects related to the SNIa light curve fitting, stretch and color correction are subdominant, see figure 2. The possibility that Cepheid calibrated SNIae to a larger extent originate in star-forming environments, thus being dimmer compared to the average Hubble flow SNIae, may bias the Hubble constant measurements has been discussed in Rigault et al. (2015).

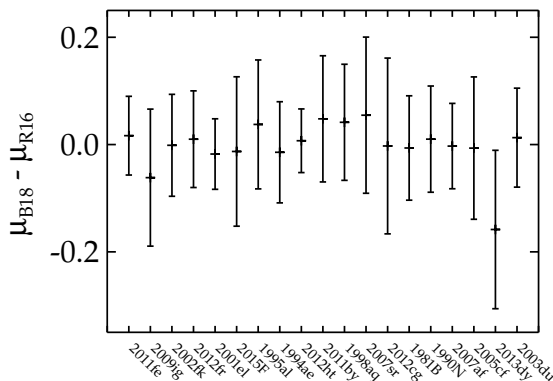


Figure 2. Comparing the distance moduli for SNIa host galaxies as derived using SNIa data from Burns et al. (2018) (B18) and Riess et al. (2016) (R16). The Cepheid data set is the same in both cases.

6. MILKY WAY PARALLAX UNCERTAINTIES

Trigonometric parallaxes potentially provide the most direct calibration of the Cepheid absolute magnitude,

M_H^W . We use data from Riess et al. (2021), with 68 MW Cepheids having estimated GAIA parallaxes. As described in Lindegren et al. (2021), there are systematic errors in the published GAIA parallax values, with the parallax bias depending on, for example, the magnitude, color and angular position of the source. Although the GAIA team provide tentative expressions for the parallax correction, given that these corrections are uncertain for sources as bright as the MW Cepheids used in this study, here, as well as in Riess et al. (2021), we will allow for the possibility of residual parallax biases to correct for. For the j th Cepheid in the MW,

$$m_{H,j}^W = \mu_j + M_H^W + b_W[P]_j + Z_W[M/H]_j. \quad (11)$$

where the distance moduli for each Cepheid is estimated using GAIA parallaxes, π , according to

$$\pi_j + zp = 10^{-0.2(\mu_j - 10)}, \quad (12)$$

where zp is a residual parallax calibration offset that we fit for together with M_H^W , b_W and Z_W by writing

$$\begin{aligned} \mu_j &= 10 - \frac{5}{\ln 10} \left[\ln \pi + \ln \left(1 + \frac{zp}{\pi} \right) \right] \\ &= 10 - \frac{5}{\ln 10} \left[\ln \pi + \frac{zp}{\pi} + \mathcal{O} \left(\frac{zp}{\pi} \right)^2 \right], \end{aligned} \quad (13)$$

effectively transforming zp into a linear parameter, and

$$\begin{aligned} m_{H,j}^W - 10 + \frac{5}{\ln 10} \ln \pi &= M_H^W + b_W[P]_j \\ &+ Z_W[M/H]_j - \frac{5}{\ln 10} \frac{zp}{\pi}. \end{aligned} \quad (14)$$

Higher order terms, $\mathcal{O}(zp/\pi)^2$, are small and corrected for in an iterative manner. So far, with the exception that we fit for zp simultaneously with all other parameters, this is similar to the approach in Riess et al. (2021).

After correcting for a constant residual parallax offset in the GAIA data, we may have a residual that correlates with magnitude and color, see figure 3. For the magnitude, we have a negative Pearson correlation of -0.15 and for the color a positive Pearson correlation 0.25 . We therefore also add corrections of the form

$$\pi \rightarrow \pi + zp_1 + zp_2 \cdot m_H + zp_3 \cdot (V - I). \quad (15)$$

Using the MW as the anchor galaxy, adding zp_2 increases the Hubble constant from $H_0 = 74.1 \pm 1.8$ to $H_0 = 77.7 \pm 2.1$. Adding also zp_3 gives $H_0 = 72.0 \pm 2.8$. The fact that a change in the parallax offset parameterization can induce a shift of $\delta H_0 = 5.7$ introduces doubt about the uncertainty estimates.

An interesting possibility for calibrating MW Cepheid distances circumventing problems connected to their

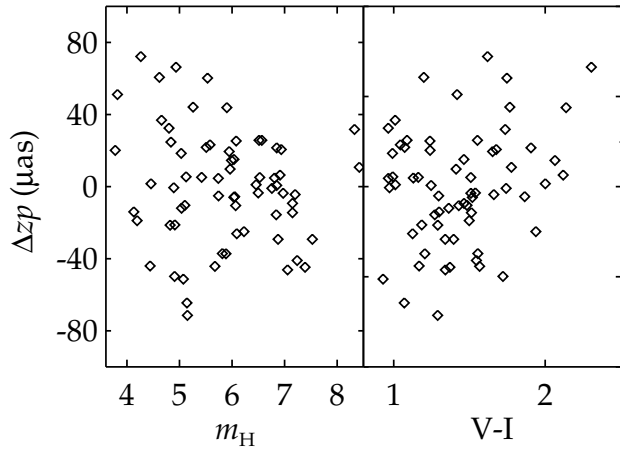


Figure 3. *Left panel:* Parallax offset residual vs H -band magnitude for MW Cepheids, with a negative Pearson correlation of -0.15 . *Right panel:* Parallax offset residual vs $V - I$ -color for MW Cepheids with a positive Pearson correlation 0.25 .

bright nature and variability is to employ Cepheids for which the distance can be estimated from the parallax of spatially resolved companions or their host open cluster. In [Breuval et al. \(2020\)](#), a sample of 36 MW Cepheids is constructed in this way, and assuming a fixed value for the GAIA calibration off-set, it was noted that the inferred H_0 is decreased comparing to the case of parallaxes measured from the Cepheids themselves. Here, we consider the impact of using the MW Cepheid sample from [Breuval et al. \(2020\)](#) when performing the full simultaneous parameter distance ladder fit, including the GAIA parallax off-set. We also find that the Hubble constant is decreased compared to using the Cepheids in [Riess et al. \(2021\)](#), and that uncertainties are increased given the smaller MW Cepheid sample size. Interestingly enough, as discussed in Section 9, this relaxes the tension between the MW and other anchors and gives $H_0 = 70.8 \pm 1.6$, in only 2.1σ tension with Planck, very similar to the result obtained when skipping MW Cepheids altogether in which case $H_0 = 71.0 \pm 1.6$ (2.1σ), even before taking other systematic uncertainties into account.

7. COLOR EXCESS DISTRIBUTIONS AND CUTS

As discussed in [Mortsell et al. \(2021\)](#), the fact that Cepheid colors and periods are correlated ([Tammann et al. 2011](#)) may cause color selection effects related to the fact that longer period Cepheids are brighter. From Figure 5, showing the different distributions of the color excess $\hat{E}(V - I)$, large variations between the different galaxies employed in the Cepheid

distance calibration are evident. This fact, possibly attributed to selection effects, may introduce systematic errors when comparing the derived Cepheid distances. MW are systematically redder compared to other anchors and SNIa host galaxies, and also have a strong correlation of long period Cepheids having larger color excesses. For each individual MW Cepheid, we compare the estimated color excess with three dimensional dust maps based on GAIA, Pan-STARRS 1 and 2MASS data where applicable ([Green et al. 2019](#); [Green 2018](#)). The generally good agreement as shown in Figure 4 confirms that the majority of the color excess is due to interstellar dust extinction, but with room for contributions from circumstellar dust and intrinsic temperature variations.

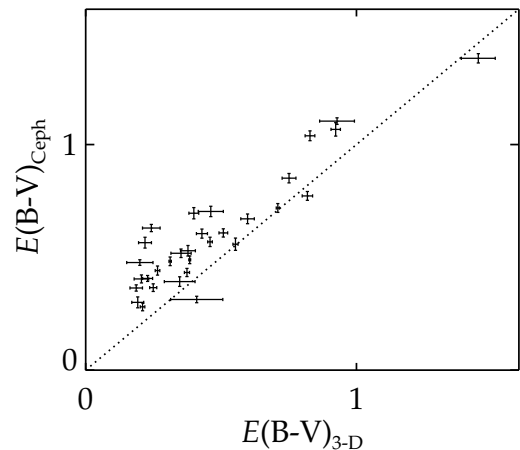


Figure 4. The $B - V$ estimated Cepheid color excess $E(B - V)_{\text{Ceph}}$ compared to the predicted dust extinction based on three dimensional (3-D) dust maps estimated following [Green \(2018\)](#).

Given that the statistical uncertainty contribution to H_0 is dominated by SNIa magnitude errors, one can afford to make rather severe cuts in the Cepheid data in order to minimize the impact of systematic effects, including color cuts to try homogenize the different color excess distributions between galaxies.

Here, we investigate the impact on H_0 of mitigating the color calibration impact by removing the reddest Cepheids, most susceptible to dust extinction. In Figure 6, we show the fitted H_0 as a function of the cut in $\hat{E}(V - I)$ we apply, when calibrating using color excesses for individual R_E with a prior. We note that the size of the error bars do not significantly increase unless $\hat{E}(V - I)_{\text{max}} \lesssim 0.1$, and that the inferred H_0 drifts towards the Planck value when cutting out redder Cepheids.

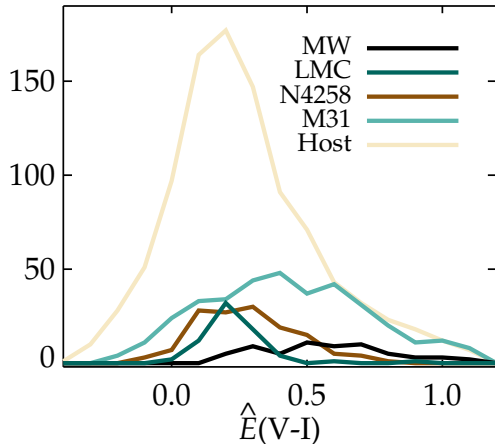


Figure 5. Distributions of estimated Cepheid color excesses $\hat{E}(V-I)$. The mean color excesses $\langle \hat{E}(V-I) \rangle$ are for the MW 0.69, for the LMC 0.28, for NGC 4258 0.33, for M31 0.50 and for the SNIa host galaxies 0.31.

Applying $\hat{E}(V-I) < 0.15$, motivated by this being the cut where statistical Cepheid uncertainties are still subdominant and we expect dust extinction not to dominate the Cepheid excess colors, we obtain $H_0 = 68.4 \pm 2.1$ for individually fitted R_E with a weak prior. Assuming a fixed global value of $R_E = 0.386$, closer in line with the analysis in [Riess et al. \(2016\)](#), we obtain $H_0 = 69.0 \pm 2.0$ for the same color cut. As evident from Figure 5, this cut effectively removes all MW Cepheids.

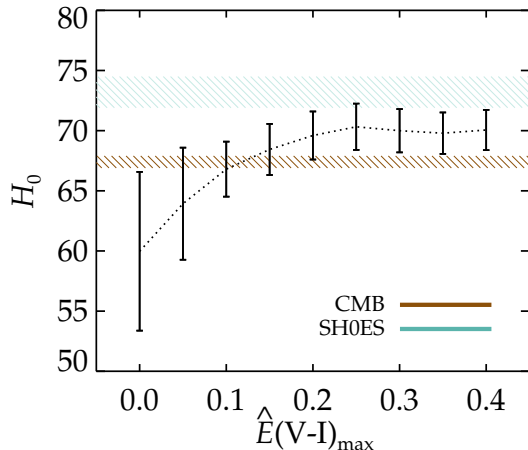


Figure 6. Fitted H_0 as a function of the cut in $\hat{E}(V-I)$ for individually fitted R_E with a weak prior. The error bars do not include intrinsic color and metallicity systematic errors.

8. RESULTS INCLUDING SYSTEMATIC ERRORS

Table 1. Individual contributions to the systematic error budget, with k and Z_\odot relating metallicities as inferred from iron and oxygen abundances as described in Section 4, Int col being Cepheid intrinsic color uncertainties as given in [Tammann et al. \(2011\)](#) and τ the intrinsic Cepheid temperature for which $\sigma_\tau = 0.02$ ([Pejcha & Kochanek 2012](#)).

Param	$\sigma(H_0)$
k	0.15
Z_\odot	0.74
Int col	0.66
τ	0.36

Finally, we also include metallicity uncertainties, as well as intrinsic color uncertainties and temperature variations by generating random Monte Carlo samples. Here, we use $k = -0.5 \pm 0.25$, $Z_\odot = 8.824 \pm 0.15$. For individual contributions to the error budget, see Table 1.

For the default calibration case, allowing for R_E to vary between galaxies, with weak prior constraints $R_E = 0.45 \pm 0.35$, we get $H_0 = 71.8 \pm 1.9$ (2.3σ)¹.

Calibrating MW Cepheid distances using companions and host clusters parallaxes following [Breuval et al. \(2020\)](#), we obtain $H_0 = 70.8 \pm 2.0$ (1.6σ), very similar to not using the MW Cepheids at all based on their sensitivity to the GAIA parallax calibration choice giving $H_0 = 70.8 \pm 2.1$ (also 1.6σ from the Planck value).

In Figure 7, we show the inferred Hubble constant from each individual anchor. It is evident that calibrating MW Cepheid distances using their own parallaxes gives a value for the Hubble constant systematically higher than the other anchors or calibrating with respect to less bright, non-variable companion sources.

Applying a color excess cut, only using Cepheids for which $\hat{E}(V-I) < 0.15$, we obtain $H_0 = 68.6 \pm 2.6$, for individually fitted R_E with weak priors, and $H_0 = 69.0 \pm 2.5$ assuming a fixed global value of $R_E = 0.386$ following [Riess et al. \(2016\)](#). We thus note that mitigating the color calibration impact by removing Cepheids for which dust extinction is expected to dominate the observed color excess, the H_0 inferred from supernovae agree with the Planck value regardless of Cepheid color calibration parameterization. It should also be noted that cutting out the blue Cepheid tail has to the opposite effect of increasing the inferred H_0 . Requiring $\hat{E}(V-I) > 0$, we obtain $H_0 = 71.9 \pm 2.1$, excluding MW Cepheids.

9. SUMMARY

¹ For the case of no R_E priors, $H_0 = 71.0 \pm 2.0$ (1.8σ).

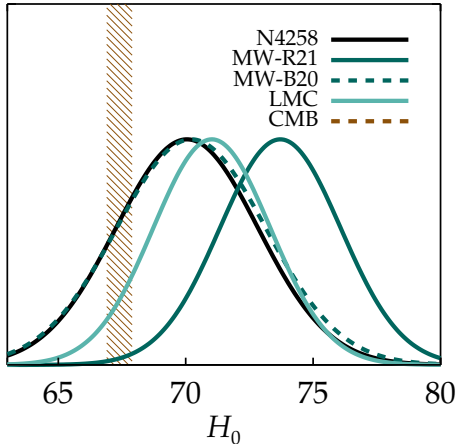


Figure 7. Results for H_0 for different anchor distances. Solid lines are fitted for individual galactic values of R_E using estimated color excesses. Note that the results are not independent, since they share the same data, except the anchor distances.

In Mortsell et al. (2021), we demonstrated the sensitivity of the Hubble constant as inferred from SNIa distances to the choice of Cepheid color calibration method. Here, we complement this analysis by investigating the impact of Cepheid temperature variations, metallicity corrections, supernova magnitude uncertainties and Milky Way parallax systematics.

The results are summarized in Figure 8. Removing MW Cepheids from the fit, for which distances have uncertainties connected to the GAIA parallax calibration, we find $H_0 = 70.8 \pm 2.1$, decreasing the difference with the Planck value to 1.6σ . This value is in agreement with $H_0 = 69.6 \pm 1.6$ obtained calibrating the absolute SNIa magnitude using the tip of the red giant branch observations (Freedman et al. 2019). A possible caveat with ours, and all other H_0 measurements using Cepheid calibrated distances, comes from the fact that the observed Cepheid color excess distribution have large vari-

ations across galaxies, and that the inferred Hubble constant is sensitive to color excess cuts in the data.

We conclude that the current Hubble tension may be an artifact of underestimating systematic effects in the calibration of the local distance ladder, including MW Cepheid distances, as well as Cepheid selection biases.

- 1 We thank Vallery Stanishev for interesting discussions
- 2 regarding stellar metallicities. EM acknowledges sup-
- 3 port from the Swedish Research Council under Dnr VR
- 4 2020-03384. AG acknowledges support from the Swedish
- 5 Research Council under Dnr VR 2020-03444, and the
- 6 Swedish National Space Board, grant 110-18.

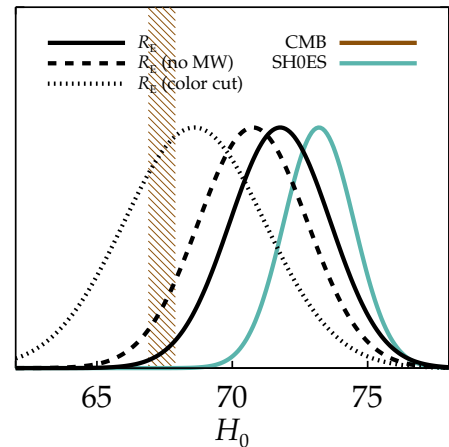


Figure 8. Comparing results for H_0 . The solid black line is for individual galactic values of R_E using color excesses, assuming prior values $R_E = 0.45 \pm 0.35$. For the dotted black line, we have imposed an upper limit on the allowed estimated color excess, only including Cepheids for which $\hat{E}(V - I) < 0.15$. For the dashed black line, we omit MW Cepheids. The solid petrol line is fitted using the Wesenheit calibration with $R_W = 0.386$ as in Riess et al. (2021) and the dashed brown region indicates the 1σ region from Planck (Aghanim et al. 2020).

REFERENCES

- Aghanim, N., Akrami, Y., Ashdown, M., et al. 2020, *A&A*, 641, A6, doi: [10.1051/0004-6361/201833910](https://doi.org/10.1051/0004-6361/201833910)
- Amarsi, A. M., Asplund, M., Collet, R., & Leenaarts, J. 2015, *MNRAS: Letters*, 454, L11–L15, doi: [10.1093/mnras/51/lv122](https://doi.org/10.1093/mnras/51/lv122)
- Betoule, M., Kessler, R., Guy, J., et al. 2014, *A&A*, 568, A22, doi: [10.1051/0004-6361/201423413](https://doi.org/10.1051/0004-6361/201423413)
- Breuval, L., Kervella, P., Anderson, R. I., et al. 2020, *A&A*, 643, A115, doi: [10.1051/0004-6361/202038633](https://doi.org/10.1051/0004-6361/202038633)
- Burns, C. R., et al. 2018, *ApJ*, 869, 56, doi: [10.3847/1538-4357/aae51c](https://doi.org/10.3847/1538-4357/aae51c)
- Follin, B., & Knox, L. 2018, *MNRAS*, 477, 4534–4542, doi: [10.1093/mnras/sty720](https://doi.org/10.1093/mnras/sty720)
- Freedman, W. L., Madore, B. F., Hatt, D., et al. 2019, *ApJ*, 882, 34, doi: [10.3847/1538-4357/ab2f73](https://doi.org/10.3847/1538-4357/ab2f73)
- Green, G. M. 2018, *The Journal of Open Source Software*, 3, 695, doi: [10.21105/joss.00695](https://doi.org/10.21105/joss.00695)

- Green, G. M., Schlafly, E., Zucker, C., Speagle, J. S., & Finkbeiner, D. 2019, *ApJ*, 887, 93, doi: [10.3847/1538-4357/ab5362](https://doi.org/10.3847/1538-4357/ab5362)
- Guy, J., Astier, P., Baumont, S., et al. 2007, *A&A*, 466, 11, doi: [10.1051/0004-6361:20066930](https://doi.org/10.1051/0004-6361:20066930)
- Israelian, G., Lopez, R. J. G., & Rebolo, R. 1998, *ApJ*, 507, 805, doi: [10.1086/306351](https://doi.org/10.1086/306351)
- Lindgren, L., Bastian, U., Biermann, M., et al. 2021, *Å*, 649, A4, doi: [10.1051/0004-6361/202039653](https://doi.org/10.1051/0004-6361/202039653)
- Luck, R. E. 2018, *The Astronomical Journal*, 156, 171, doi: [10.3847/1538-3881/aadcac](https://doi.org/10.3847/1538-3881/aadcac)
- Madore, B. F. 1982, *ApJ*, 253, 575, doi: [10.1086/159659](https://doi.org/10.1086/159659)
- Mortsell, E., Goobar, A., Johansson, J., & Dhawan, S. 2021, *The Hubble Tension Bites the Dust: Sensitivity of the Hubble Constant Determination to Cepheid Color Calibration*. <https://arxiv.org/abs/2105.11461>
- Paczynski, B. 1996. <https://arxiv.org/abs/astro-ph/9608094>
- Pejcha, O., & Kochanek, C. S. 2012, *ApJ*, 748, 107, doi: [10.1088/0004-637x/748/2/107](https://doi.org/10.1088/0004-637x/748/2/107)
- Pietrzyński, G., Graczyk, D., Gellenne, A., et al. 2019, *Nature*, 567, 200–203, doi: [10.1038/s41586-019-0999-4](https://doi.org/10.1038/s41586-019-0999-4)
- Reid, M. J., Pesce, D. W., & Riess, A. G. 2019, *ApJ*, 886, L27, doi: [10.3847/2041-8213/ab552d](https://doi.org/10.3847/2041-8213/ab552d)
- Riess, A. G., Casertano, S., Yuan, W., et al. 2021, *ApJ*, 908, L6, doi: [10.3847/2041-8213/abdbaf](https://doi.org/10.3847/2041-8213/abdbaf)
- Riess, A. G., Casertano, S., Yuan, W., Macri, L. M., & Scolnic, D. 2019, *ApJ*, 876, 85, doi: [10.3847/1538-4357/ab1422](https://doi.org/10.3847/1538-4357/ab1422)
- Riess, A. G., et al. 2016, *ApJ*, 826, 56, doi: [10.3847/0004-637X/826/1/56](https://doi.org/10.3847/0004-637X/826/1/56)
- Rigault, M., Aldering, G., Kowalski, M., et al. 2015, *The Astrophysical Journal*, 802, 20, doi: [10.1088/0004-637x/802/1/20](https://doi.org/10.1088/0004-637x/802/1/20)
- Tammann, G. A., Reindl, B., & Sandage, A. 2011, *A&A*, 531, A134, doi: [10.1051/0004-6361/201016382](https://doi.org/10.1051/0004-6361/201016382)
- Vagnozzi, S. 2019, *Atoms*, 7, 41, doi: [10.3390/atoms7020041](https://doi.org/10.3390/atoms7020041)
- von Steiger, R., & Zurbuchen, T. H. 2015, *ApJ*, 816, 13, doi: [10.3847/0004-637x/816/1/13](https://doi.org/10.3847/0004-637x/816/1/13)